Materials Science & Engineering A 614 (2014) 96–105

Contents lists available at ScienceDirect

Materials Science & Engineering A

journal homepage: www.elsevier.com/locate/msea

Optimization of strength by microstructural refinement of MgY_2Zn_1 alloy during extrusion and ECAP processing

G. Garces *, M.A. Muñoz-Morris, D.G. Morris, P. Perez, P. Adeva

Department of Physical Metallurgy, CENIM-CSIC, Avenida Gregorio del Amo 8, E-28040 Madrid, Spain

ARTICLE INFO

Article history:
Received 27 May 2014
Received in revised form
1 July 2014
Accepted 7 July 2014
Available online 15 July 2014

Keywords:
Magnesium alloys
ECAP
Mechanical property
LPSO phase

ABSTRACT

A MgY_2Zn_1 alloy composed of a Mg matrix and about 19% of LPSO phase has been prepared by casting and further processing at high temperature by extrusion and equal channel angular pressing (ECAP). After extrusion an elongated microstructure was obtained in the direction of extrusion where the LPSO phase appears partially broken and the Mg matrix is partially recrystallized to very fine grain size. ECAP processing carried out both in the as-cast and extruded alloy leads to further grain refinement by recrystallization and also to further comminution of the LPSO particles. The increase in strength of the alloy by the different processing routes has been analysed in terms of the contributions from the LPSO particles and the deformed and the recrystallized grains in the magnesium matrix.

1. Introduction

Mg-transition metals-Y/Rare Earth alloys containing Long-Period Stacking Ordered structures (LPSO) are very attractive for structural applications due to the combination of low density with high mechanical strength, appreciable ductility and good creep resistance [1–12]. LPSO phases are solid solutions of yttrium or rare earth elements and transition metals in the magnesium lattice, where these atoms are arranged periodically in magnesium basal planes forming ordered structures [13–16]. The Mg–Y–Zn system has received special attention, and much research has been devoted to improving the mechanical strength of the alloys, with greatest interest in the alloy MgY_2Zn_1 (at%) where a strength of 610 MPa with 5% of elongation at room temperature was obtained by warm extrusion of rapidly solidified ribbons [1]. Such high strength was attributed to the coexistence of fine, 100–200 nm, magnesium grains with a distribution of LPSO phase particles at grain boundaries. However, rapid solidification techniques are expensive and also high temperature consolidation techniques are required to obtain bulk material, leading to microstructure coarsening.

Recently, Yamasaki et al. [7] have carried out extrusion experiments of a $Mg_{97}Y_2Zn_1$ alloy obtaining a yield stress of 350 MPa and 8% ductility by controlling the extrusion microstructure, characterized by a mixture of fine, randomly oriented, recrystallized α-Mg grains, hot worked coarse α-Mg grains, with strong basal texture, and fiber-shaped LPSO phase. They suggested that the fine magnesium grains contribute to ductility improvement while the textured coarse α-Mg grains as well as the LPSO phase contribute to the mechanical strength of the alloy. The contribution of the LPSO phase in the alloy can be considered as a reinforcement in a metal matrix composite since the Young´s modulus of the LPSO is two to three times higher than that of the magnesium matrix [17,18]. Hagihara et al. [8] carried out a detailed study of strengthening mechanisms in a $Mg_{97}Y_2Zn_1$ alloy after extrusion at 450 °C followed by anneals at different temperatures with the aim of obtaining a variable grain size. They identified a Hall–Petch type contribution of grain size to strengthening in addition to the reinforcement effect due to the LPSO phase.

Severe plastic deformation (SPD) techniques have emerged in the past decade as effective methods for the production of bulk metallic materials with very fine grain sizes [19–22]. Among such techniques, equal channel angular pressing (ECAP) has been used in magnesium alloys containing LPSO phases inducing their fracture as well as grain refinement [23–29], improving mechanical strength and favouring superplastic forming. To optimize the mechanical properties of the alloys, however, it is necessary to quantify the contributions from each microstructural parameter to strength and ductility in order to select the most adequate processing technique for the desired microstructure.

In the present study an MgY_2Zn_1 alloy has been processed by a combination of extrusion and ECAP at two different temperatures and the microstructural changes taking place have been quantified. These changes have been related to the mechanical properties obtained to understand the specific contributions to strengthening of the recrystallized and the deformed magnesium grains as well as from the reinforcing LPSO phase.

* Corresponding author. Tel.: +34 91 553 8900; fax: +34 91 534 7425.
E-mail address: ggarces@cenim.csic.es (G. Garces).

http://dx.doi.org/10.1016/j.msea.2014.07.012
0921-5093/

2. Experimental

The alloy used had a nominal composition of 97%Mg–2%Y–1% Zn (atomic per cent) and was prepared by melting in an electric resistance furnace using high purity Mg and Zn elements and a Mg–22%Y master alloy. Ingots were cast by pouring the liquid metal into a cylindrical steel mould of diameter 42 mm. The alloy was homogenized at 350 °C for 24 h and then extruded to a round bar at 350 °C using extrusion ratios of 4:1(R4, total strain 1.4) and 18:1 (R18, total strain 2.9), respectively. The extrusion rate was 30 mm/min. Also the homogenized cast alloy was processed by ECAP at 350 °C. For this, the cast bars were machined into cylinders of 20 mm in diameter, 70 mm long, and processing was carried out in a hydraulic machine using a circular cross-section die of diameter 20 mm with die angle of 118°, producing a true strain of 0.7 per pass. For ECAP at 350 °C both routes A and B were used [30,31], i.e., with either no rotation or a 90° rotation of sample between passes, respectively. Using route A it was possible to process up to 12 passes without any cracking of samples. For ECAP at 300 °C the alloy was previously extruded at 350 °C with a ratio of 4:1 (R4) to a bar of diameter 20 mm. In this state it was possible to process up to eight passes using route A. This route was maintained since various studies examining the severe plastic deformation of metals and metal–matrix composites have suggested that route A may lead to faster matrix grain size refinement [21,32,33]. For ECAP, samples were heated in the die, reaching die temperature in 5 min before pressing. At the standard pressing speed used in all cases (20 mm/min) the total cycle time (preheating and pressing) was 10 min. Following each ECAP pass, the heated split-die was opened hydraulically for rapid sample removal and water quenching.

Microstructures were examined by optical microscopy (OM) and scanning electron microscopy (SEM). Samples were prepared by mechanical polishing and finishing with an etching solution of 5 ml acetic acid, 20 ml water and 25 ml picric acid in methanol. Quantitative image analysis was carried out to follow the evolution of fraction recrystallized and grain size in the magnesium matrix after extrusion or during successive ECAP passes. For the recrystallized fraction several SEM images from areas recrystallized to different extents were measured to give a good statistical measure of this fraction. The sizes of recrystallized grains were measured counting a minimum of 500 grains from images taken using backscattered electrons in the SEM. Statistical analyses were carried out with the software Sigma Scan Pro and taking the grain size as the average value obtained.

The mechanical properties of the alloy in all conditions were evaluated by tensile testing cylindrical samples of diameter 3 mm and gauge length 10 mm. The material obtained after processing by eight ECAP passes at 300 °C had poor ductility, and hence compression tests were carried out to determine the flow stress, using cylinders 3 mm in diameter and height 5–6 mm. Both types of tests were carried out using a universal testing machine at a strain rate of $4 \times 10^{-4}\,s^{-1}$. All the samples were tested along the direction of extrusion or ECAP processing, with two to three samples examined for each material condition.

3. Results

3.1. Mechanical properties

Fig. 1 shows stress–strain curves illustrating the behaviour of the materials when tested in tension for the various conditions of processing. The shape of the curves was similar for all states, with high work hardening over the first about 1–2% strain, but then falling to low values. Also we note that the materials with the highest ductility (about 10%) were obtained by processing at 350 °C, both by extrusion (R18) and after 12 ECAP passes in the as-cast state. During ECAP processing the route used did not appear to affect the strength of the material whilst the processing temperature was the most significant parameter determining the final strength of the alloy.

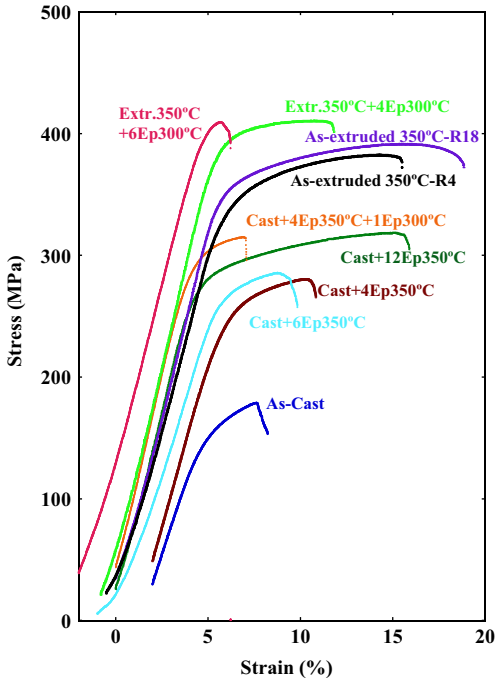

Fig. 1. Stress–strain curves of the materials obtained when tested in tension for the various conditions of processing.

Fig. 2 shows the evolution of the yield stress (flow stress at 0.2% plastic strain) ultimate tensile strength (UTS) and ductility determined from the stress–strain curves of Fig. 1 for all the alloy conditions. In Fig. 2a the values of yield stress are plotted as a function of the total processing strain for each alloy condition where we note that for an equivalent strain of 2.9 the yield stress of the extruded alloy R18 is lower than the values obtained after ECAP at 300 °C. Also in the same figure we see the increase in yield stress obtained when the cast alloy processed four ECAP passes at 350 °C is given an additional pass (strain 3.5) at 300 °C. This value, 281 MPa, is, however, not reached when processing at 350 °C even up to 12 passes (strain 8.4). The values are also shown in Table 1 where we note that the initial flow stress of 140 MPa of the as-cast alloy increases steadily with the increase in the number of ECAP passes at 350 °C until a value of 264 MPa is reached for 12 passes. The flow stress of the alloy extruded at 350 °C is slightly higher with values of 325 and 342 MPa for the extrusion ratios R4 and R18, respectively. The highest values of 392 and 418 MPa are obtained after six and eight passes, respectively, of ECAP processing at 300 °C.

In Fig. 2b and also in Table 1 we show the values of ultimate tensile strength and ductility in tension. The best ductilities are obtained after extrusion or ECAP processing at 350 °C (10%), while decreasing the processing temperature to 300 °C reduces the ductility to 6% and 1.5% after four and six passes, respectively, and zero after eight passes. In this condition, however, the alloy exhibits work hardening in compression such that we measure an increase of 100 MPa at 6% compressive strain.

3.2. Microstructure evolution

Figs. 3 and 4 show backscattered electron images of microstructural evolution observed in the as-cast alloy and after extrusion or

ECAP processing, illustrating the changes that take place in the distribution and morphology of the LPSO phase (brighter) within the magnesium matrix. As already studied by several authors [11,17,34] in the as-cast state (Fig. 3a) this type of alloy has an equiaxed dendritic microstructure consisting of magnesium dendrites (darker) and dendrite walls occupied by the LPSO phase (brighter). In the present alloy the dendrite size is about 30–50 μm and the volume fraction of LPSO phase measured was 19 ± 2%. ECAP processing modifies this distribution by deforming and breaking the LPSO phase to different extents depending on the total processing strain and temperature. In this way we see in Fig. 3b and c that after four (strain 2.8) and 12 (strain 8.4) ECAP passes at 350 °C the microstructure appears elongated in the direction of shear, the effect being more pronounced with the increase in total strain. This change in morphology is more evident after extrusion with a ratio of 18:1 (Fig. 3d) where the LPSO appears very elongated in the direction of extrusion even though the total strain is only 2.9. As these distribution changes are taking place, the LPSO is broken down into finer pieces which remain, nevertheless, agglomerated (Fig. 3e and f). Fig. 4 shows examples of the elongated distributions obtained after extrusion with a ratio of 4:1 (strain 1.4), Fig. 4a, and followed by eight ECAP passes at 300 °C, Fig. 4b. Even though at these low magnifications there appears little difference between the microstructures, the higher magnification images of Fig. 4c and d indicate that the major difference lies in the extent of comminution of the LPSO phase which has only partially occurred after extrusion but is generalized after eight passes of ECAP at the lower temperature.

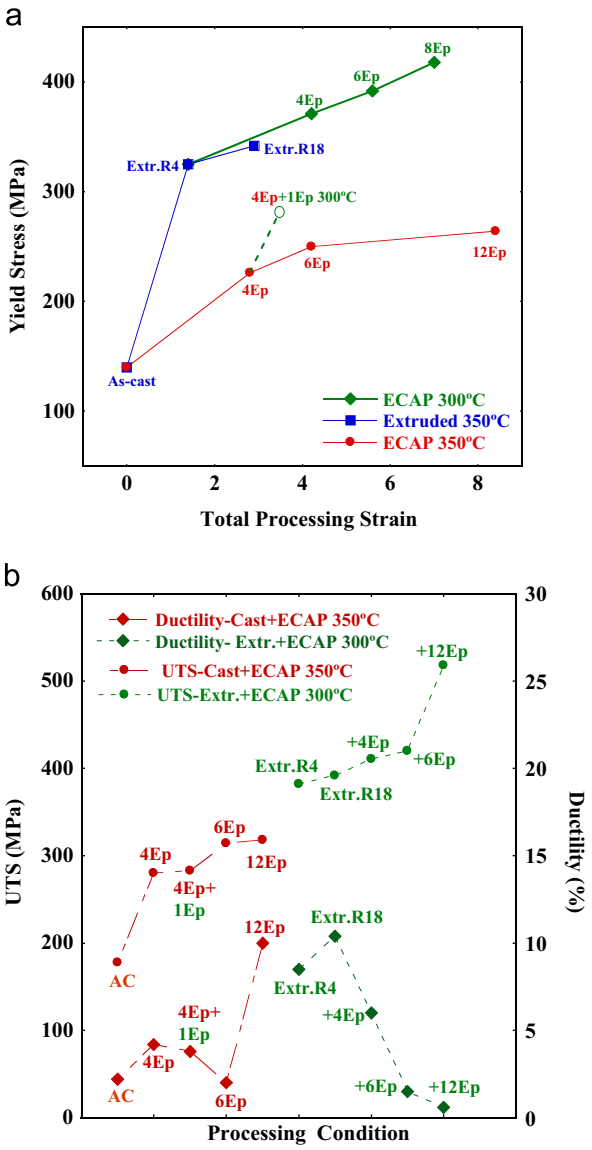

Fig. 2. (a) Evolution of yield stress with amount of total processing strain for all alloy conditions. (b) Evolution of ultimate tensile strength and ductility measured for the different processing conditions.

During the high temperature processing, both extrusion and ECAP, dynamic recrystallization (DRX) of the magnesium matrix takes place, the extent of which increases with increasing deformation. Fig. 5 illustrates examples of different recrystallized zones used to measure recrystallized volume fractions. Fig. 5a shows a zone only slightly recrystallized while in b the fraction recrystallized is almost 50%, from the samples extruded R4 or R18. Several such zones were taken to quantify the recrystallized volume fractions ($Fv_{recryst.}$) given in Table 1. In Fig. 5c and d we show examples of such recrystallization observed in the materials processed in the cast state after four or 12 ECAP passes, respectively. The major feature in the recrystallization process is that it always started in contact with the LPSO particles, as evidenced in Fig. 5a and c indicating that strain accumulation at those interfaces enhances dynamic recrystallization.

As seen in Table 1 and Fig. 6, the average recrystallized volume fraction at 350 °C increases with processing strain from 25% after four ECAP passes in the as-cast state to 73% after 12 passes. In the extruded alloy (R4) prior to ECAP the average recrystallized fraction was 32% increasing to 50% after eight passes ECAP at 300 °C. This value is, however, lower than the 65% obtained in the extruded alloy R18 to a total strain of 2.9 at 350 °C. Such higher dependence of the recrystallized fraction on strain in the materials extruded at 350 °C is visualized in Fig. 6.

The SEM images of Fig. 7 illustrate examples of the recrystallized grains used to quantify the grain size distributions shown in the histograms of Fig. 8. In Table 1 we have listed the average recrystallized grain sizes measured from such histograms which range from

Table 1
Total processing strain, ε_T, volume fraction magnesium recrystallized, $Fv_{recryst.}$, recrystallized grain size, $D_{Mg\ recryst}$, yield stress, $\sigma_{0.2}$, ultimate tensile strength, UTS, and tensile ductility for the present MgY_2Zn_1 alloy in the as-cast state and after all processing conditions. Calculated strengthening contributions due to grain refinement, σ_{HP}, and deformed grains, $\sigma_{def.}$, are also shown. See text for details.

Alloy condition	ε_T (%)	$Fv_{recryst.}$ (%)	$D_{Mg\ recryst.}$ (μm)	$\sigma_{0.2}$ (MPa)	UTS (MPa)	Ductility (%)	σ_{HP} (MPa)	$\sigma_{def.}$ (MPa)
As-cast	–	–	30–50	140	178	2.2	–	–
Cast + 4Ep350 °C-rB	2.8	25	1.1	226	280	4.2	179	93
Cast + 4Ep350 °C + 1Ep300 °C-rB	3.5	30	0.9	281	314	2.0	198	175
Cast + 6Ep350 °C-rB	4.2	39	1.3	250	283	3.8	165	133
Cast + 12Ep350 °C-rA	8.4	73	1.5	264	318	10	153	186
As-extruded 350 °C-R4	1.4	32	1.2	325	382	8.5	172	267
As-extruded 350 °C-R-18	2.9	65	0.90	342	392	10.4	198	375
Extr. 350 °C + 4Ep300 °C-rA	4.2	38	0.62	371	411	6	240	328
Extr. 350 °C + 6Ep300 °C-rA	5.6	42	0.63	392	420	1.5	237	378
Extr. 350 °C + 8Ep300 °C-rA	7	50	0.65	418	518	–	233	477

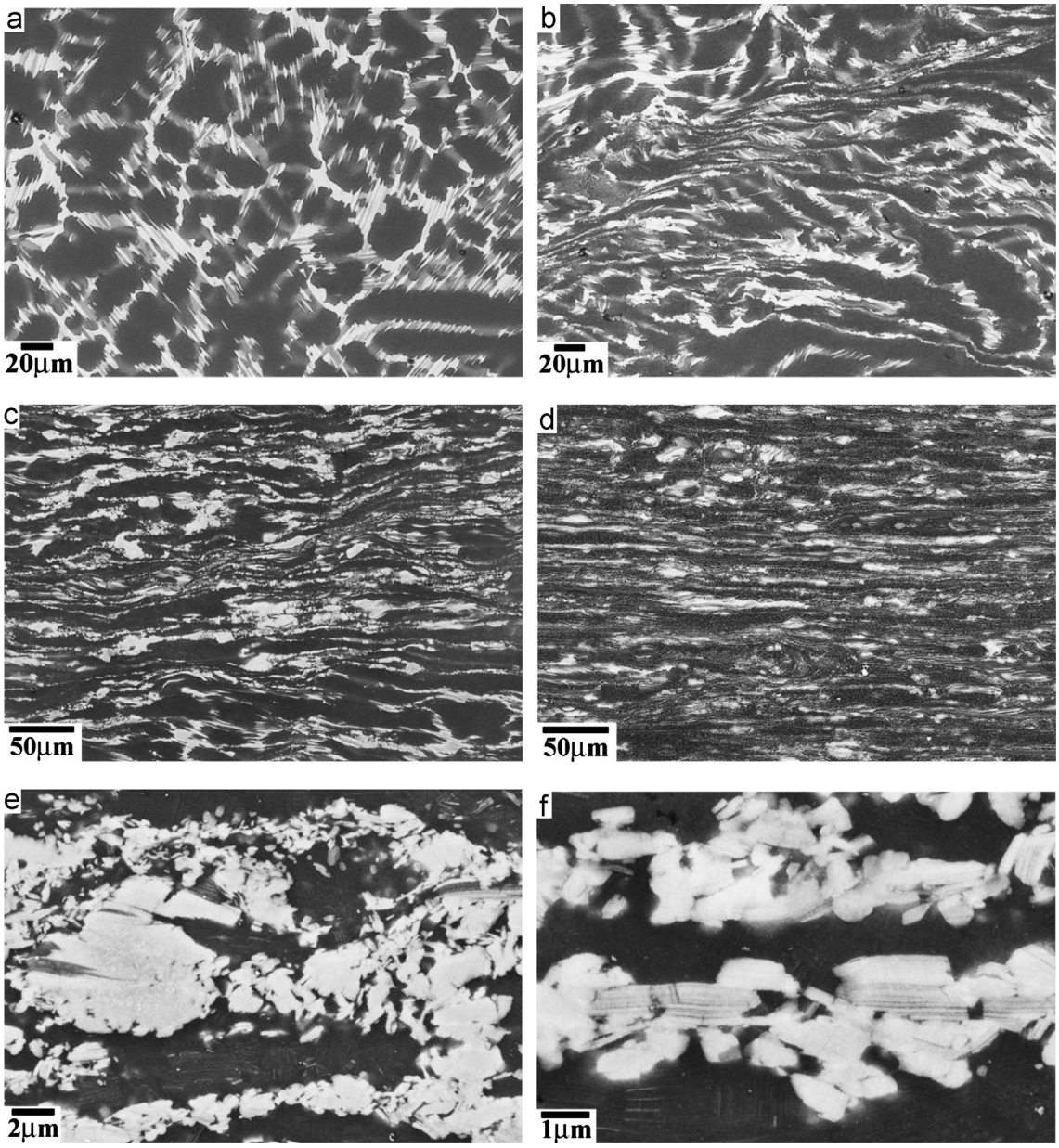

Fig. 3. Backscattered electron images illustrating the changes in the distribution and morphology of the LPSO phase (brighter) within the magnesium matrix. (a) As-cast alloy, (b) and (c) after four and 12 ECAP passes at 350 °C in cast state, respectively, (d) as extruded R18 at 350 °C; (e) and (f) higher magnification details from the broken LPSO phase taken from (c) and (d) after 12 passes ECAP and extrusion R18 at 350 °C, respectively.

1.2 to 0.9 μm in the as-extruded materials and 1.1 to 1.5 μm after four and 12 ECAP passes at 350 °C. The smallest grain sizes (620–650 nm) were measured in the materials processed by ECAP at 300 °C which before ECAP had an initial value of 1.2 μm in the extruded R4 state. Fig. 9 shows the evolution of grain size as a function of total strain for all the material conditions. It is worth noting that, as confirmed by Yamasaki et al. [7], the new dynamically recrystallized (DRX) grains have random orientations while the remaining deformed grains have a strong texture with basal planes parallel to the direction of extrusion.

4. Discussion

4.1. Microstructural evolution during processing

The microstructure changes taking place during extrusion and ECAP depend mainly on temperature and total strain during processing. As already confirmed in previous studies by several authors, the extrusion process leads to the elongation of the equiaxed dendritic microstructure along the extrusion direction [17,35,36]. The LPSO phase is highly deformed by kinking [5,35–39]. However, other authors have not mentioned that during the extrusion process the LPSO is also cracked and comminuted to a certain extent as evidenced in Figs. 3f and 4d. This elongated microstructure of agglomerated comminuted LPSO particles is most typical of the extruded R18 material (Fig. 3d). For an equivalent processing strain of 2.8, the material processed by four ECAP passes at 350 °C in the cast state (Fig. 3b) shows the LPSO phase not to be deformed or broken down so much, but after 12 ECAP passes at that temperature the comminution is well generalized (see Fig. 3e). This is believed to be caused by the slower strain rate of the ECAP shearing as well as the possibility of relaxation between passes and, as a consequence, a much higher processing strain is required to fracture and finally comminute the LPSO phase. For ECAP at the lower temperature of 300 °C, however, the samples used were first extruded at 350 °C to a low ratio

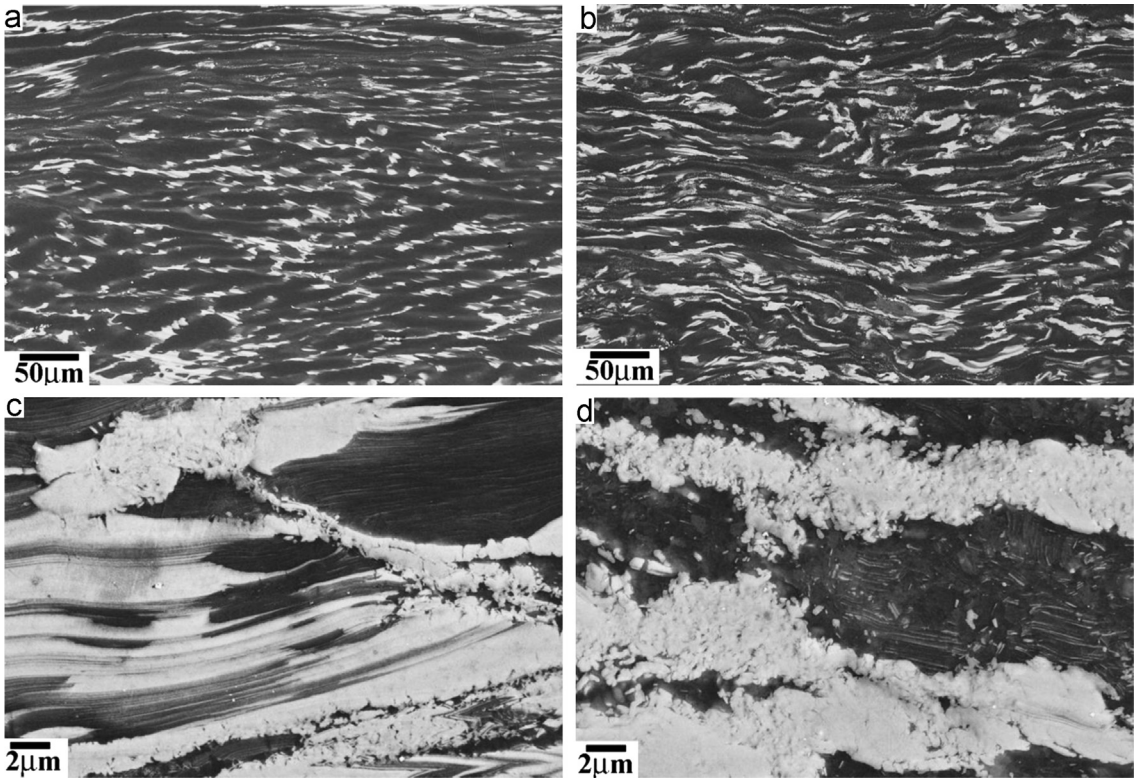

Fig. 4. Backscattered electron images showing the distribution and morphology of the LPSO phase (brighter) within the magnesium matrix. (a) and (c) as extruded R4 at 350 °C and corresponding higher magnification detail; (b) after eight ECAP passes at 300 °C in extruded state and (d) corresponding higher magnification detail (see text for details).

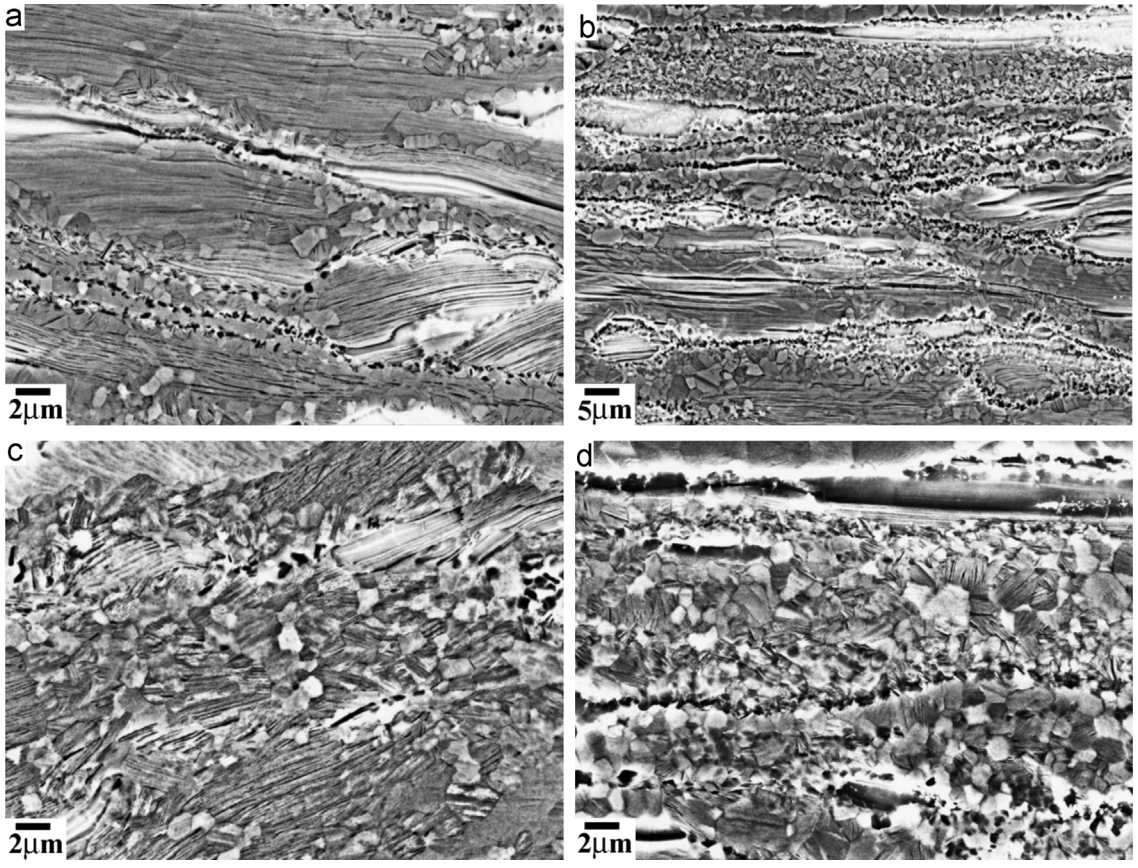

Fig. 5. Examples illustrating the different extent of dynamic recrystallization taking place in the magnesium matrix under different conditions of high temperature processing (a) and (b) as extruded R4 and R18 at 350 °C, respectively; (c) and (d) after four and 12 ECAP passes at 350 °C in the cast state, respectively.

(R4, equivalent strain 1.4) where the microstructure was only slightly elongated (Fig. 4a) and the LPSO only partially fractured (Fig. 4c). After the eight ECAP passes (total strain 7) at 300 °C the comminution of the LPSO phase was almost complete (Fig. 4d) and the microstructure was elongated along the shear direction. Thus, similar microstructures are obtained in the cast sample processed by 12 ECAP passes at 350 °C (total strain 8.4) and in the extruded R4 sample processed by eight passes at 300 °C (total strain 7). This indicates that the lower temperature compensates the higher processing strain because recovery processes are less effective leading to a faster accumulation of stress concentrations at the LPSO particle interfaces, which are required to deform and, eventually, fracture the particles.

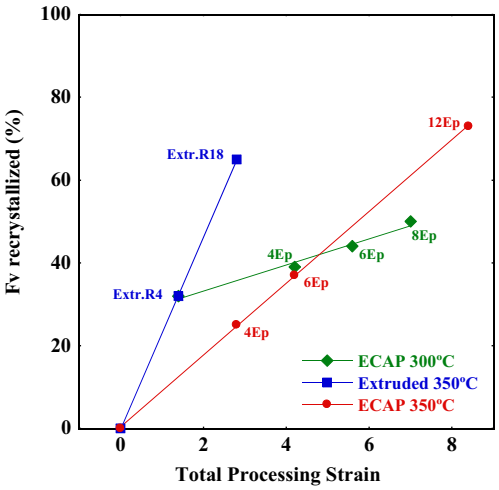

Fig. 6. Plot of the recrystallized fraction measured in the magnesium matrix as a function of the total processing strain for all the conditions.

In parallel with the comminution of the LPSO phase into short fiber-shaped particles the magnesium matrix transforms into a bimodal microstructure by DRX, the extent of which also depends on temperature and total strain during processing, see Fig. 5. In this figure we note that the DRX process always starts at the particle–matrix interfaces where the stress concentrations are accumulated due to the incompatibility of deformation between the two phases. The plots shown in Fig. 6 confirm a linear dependence of fraction recrystallized with total processing strain under all conditions of processing, with slopes that are three and eight times higher during extrusion than during ECAP at 350 °C and 300 °C, respectively.

At the same time the size of the DRX grains is much smaller after ECAP at 300 °C than at 350 °C even though higher strains were reached at the higher temperature (see Table 1 and Fig. 9). Also in Fig. 9 we confirm that extrusion at 350 °C leads to a smaller grain size, for the same equivalent strain, than ECAP at the same temperature. This has been attributed to the longer exposure time at 350 °C during ECAP, necessary to produce several passes to reach the total strain, which enhances grain growth. This is also confirmed by the continuous increase in grain size observed between four and 12 ECAP passes at 350 °C. On the other hand, the grain size decrease observed during increasing strain by extrusion at 350 °C follows the same line as that between extrusion R4 and four ECAP passes at 300 °C. This means that an increase of 1.4 strain at 350 °C during extrusion is equivalent to an increase of 2.8 strain by ECAP at 300 °C with respect to the driving force required for nucleation and growth of the new grains during DRX.

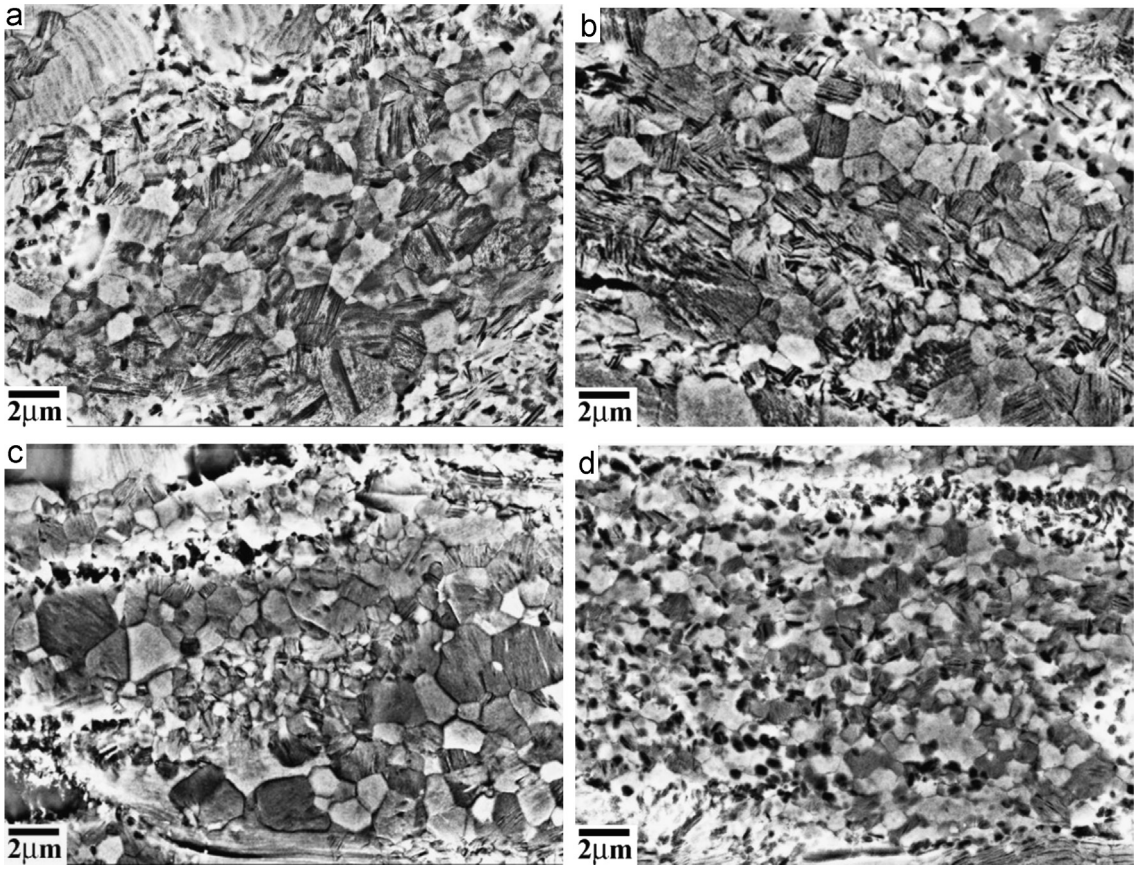

Fig. 7. Backscattered electron images showing examples of recrystallized magnesium grains from which grain sizes were measured. (a) After four passes ECAP at 350 °C in cast state; (b) and (c) as extruded R4 and R18 at 350 °C, respectively; (d) after eight ECAP passes at 300 °C in the extruded state.

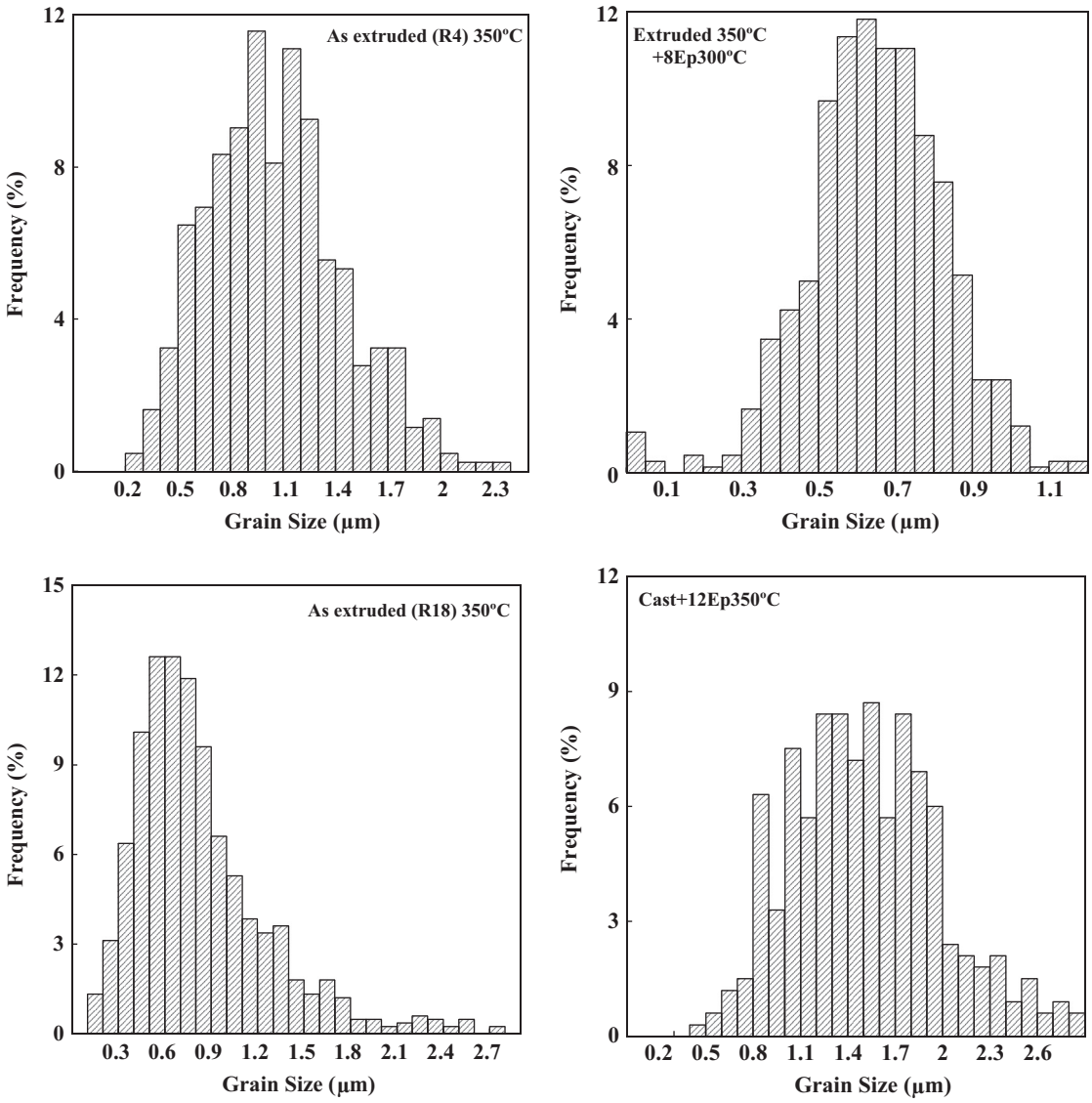

Fig. 8. Examples of histograms showing the distributions of grain size measured.

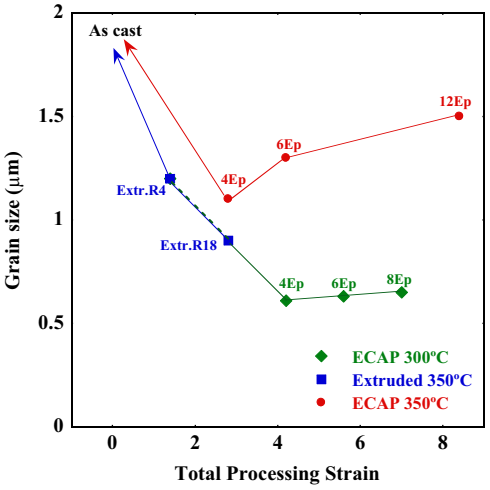

Fig. 9. Plot of grain size evolution as a function of total processing strain for the different alloy conditions.

4.2. Analysis of mechanical properties

Examination of Figs. 1 and 2 confirms that thermomechanical processing by extrusion and/or ECAP improve the mechanical properties of the cast MgY_2Zn_1 alloy, in particular the yield strength and the UTS values, but also the ductility from the low value of the as-cast state. Increased UTS is related to the total work hardening and ductility achieved in tension which, as seen by the tensile curves of Fig. 1, exhibit very similar shape for the different processing conditions. Although the maximum ductilities (between 8.5 and 10.4) were obtained in the extruded samples, both R4 and R18, and after 12 ECAP passes at 350 °C, the maximum values of UTS were obtained for the materials processed by ECAP at 300 °C, with lower ductility but higher yield stress (see Fig. 2b), indicating that there is a maximum work hardening capacity that the processed materials can accumulate after yielding. This strengthening behaviour has been related to the different microstructural aspects already described in the previous section which contribute to different extents to the total hardening capacity of the material. One of these aspects is the total volume fraction of LPSO phase which appears fractured and comminuted after

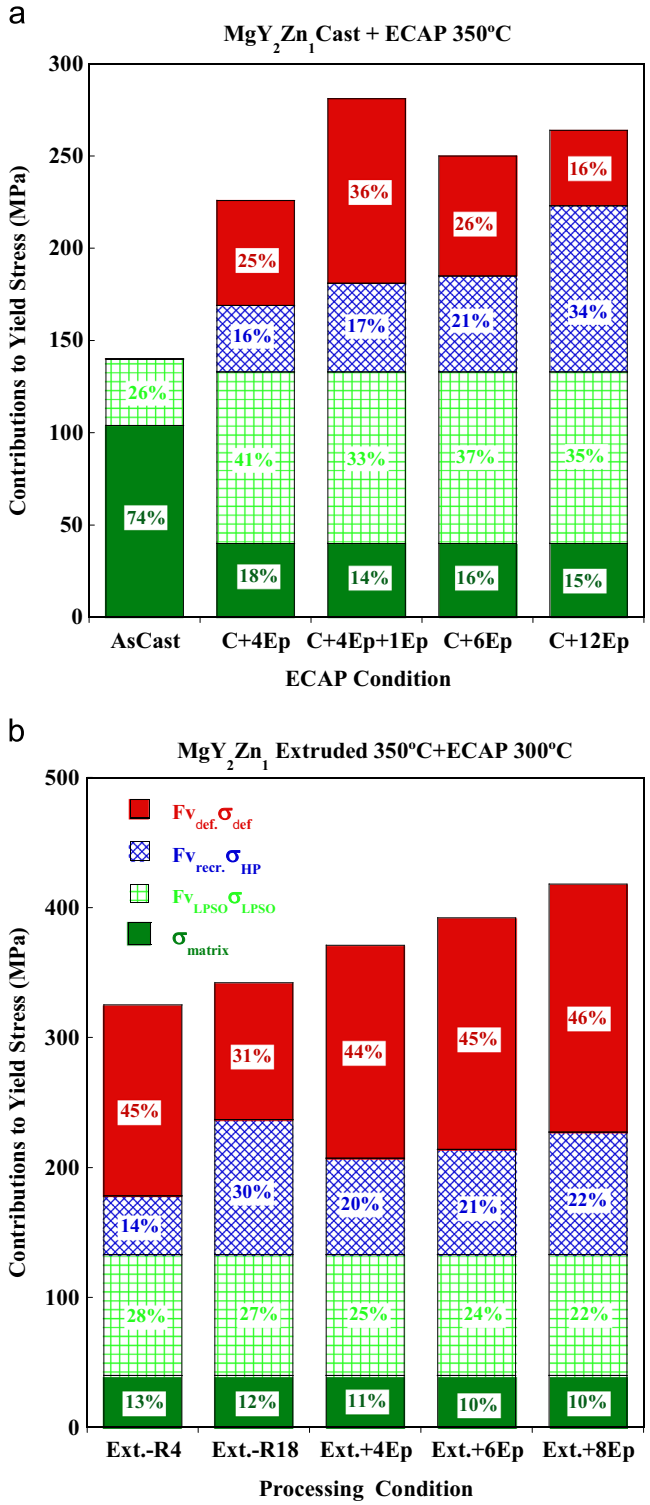

Fig. 10. Plots of strengthening contributions from the different microstructural parameters for all alloy conditions. As-cast materials (C) were processed by ECAP at 350 °C (in one case by 4 ECAP passes at 350 °C and 1 ECAP pass at 300 °C). Extruded material R4 was subsequently processed by ECAP at 300 °C. See text for details.

processing, indicating that the stress localization at the magnesium/LPSO interfaces accumulates until a maximum value is reached at which stress transfer occurs. The second aspect is the different fractions of recrystallized magnesium matrix areas that also nucleate at the interface with the LPSO phase due to the stress incompatibilities. The third aspect is the grain refinement achieved in those recrystallized zones which will determine the extent of the corresponding strengthening. In what follows we have taken into account all these parameters to analyse the total strengthening achieved in the processed materials.

For the analysis we have used the same approach as that of a previous study made in the same MgY_2Zn_1 alloy by Hirano et al. [35] after extrusion at different temperatures and strain rates. The authors considered the processed materials as composites consisting of a mixture of randomly oriented magnesium grains, deformed magnesium grains with strong basal texture, and fiber-shaped LPSO phase. In this study we have analysed the yield stress of the as-cast alloy with a model of strengthening, based on the shear lag theory [40,41], whereby a composite of hard LPSO phase particles and soft Mg matrix yields when the matrix deforms plastically, with the particles forcing the surrounding matrix to deform locally more extensively. Oñorbe et al. [18] have demonstrated experimentally the load transfer mechanism between the magnesium matrix and the elongated LPSO particles. Load transfer to the particles will depend on the difference of elastic moduli at the interface [42] and the local changes of matrix microstructure [43]. The yield stress, $\sigma_{0.2}$, of the composite is given by

$$\sigma_{0.2} = f_{vm}\sigma_m + f_{vp}\sigma_{LPSO} \quad (1)$$

where f_{vm} is the volume fraction of magnesium matrix (81%), f_{vp} is the volume fraction (19%) of LPSO particles and σ_m and σ_{LPSO} are the stresses carried by the matrix and the particles at yielding of the composite. We have measured the yield stress, σ_{LPSO}, of the LPSO phase in compression using a single phase cast $Mg_{98}Y_7Zn_5$ alloy, with the same 18R structure, and we have obtained a value of 190 MPa. Substituting in Eq. (1) values corresponding to the as-cast alloy we obtain

$$40 = 0.81\sigma_m + 0.19 \times 190 \quad (2)$$

from which we deduced a value of the stress carried out by the magnesium matrix, $\sigma_m = 128$ MPa. This means that in the as-cast alloy the matrix contributes 74% of the total composite strength while the LPSO phase, with a smaller volume fraction, contributes with 26% of the total strength, see Fig. 10a. It should be noted that in the as-cast alloy the matrix strength contains two contributions, $\sigma_m = \sigma_0 + \sigma_{SS}$, the value σ_0 corresponding to the intrinsic stress of the Mg matrix, and σ_{SS} to any strengthening due to a solid solution effect. The latter, however, should be close to zero in the heat treated processed materials.

After processing, the term σ_m contains three contributions, namely, the intrinsic stress, σ_0, of the Mg matrix, the one due to the fraction of DRX magnesium grains, f_{vrecr}, σ_{HP}, and that due to the fraction of deformed magnesium grains, $(1-f_{vrecr.})\,\sigma_{def.}$. Hence Eq. (2) can be rewritten as

$$\sigma_{0.2} = f_{vm}\sigma_m + f_{vp}\sigma_{LPSO} = 0.81[s_0 + f_{vrecr.}\sigma_{HP} + (1-f_{vrecr.})\sigma_{def.}] + f_{vp}\sigma_{LPSO} \quad (3)$$

For the value of σ_{LPSO} after extrusion we have measured, both in tension and compression, the yield stress of the extruded single phase alloy ($Mg_{98}Y_7Zn_5$) and we have obtained an average value $\sigma_{LPSO} = 490$ MPa [44]. We have also determined the values of σ_0 and σ_{HP} based on a study made by Hagihara et al. [8] in the same MgY_2Zn_1 alloy after extrusion and heat treatments. They analysed the dependence of yield stress on the size of DRX magnesium grains and obtained a linear Hall–Petch relationship, $\sigma_{HP} = \sigma_0 + K_{HP}/D^{1/2}$, from which they deduced the slope of the line as $K_{HP} = 188$ MPa $\mu m^{-1/2}$ and the intercept on the ordinate as $\sigma_0 = 49$ MPa. Using the same Hall–Petch constant, K_{HP}, and the values of the recrystallized grain sizes, $D_{Mg\ recrist.}$, together with the recrystallized fractions, $f_{vrecr.}$, measured in our present study we have deduced the contributions to the yield stress from the recrystallized magnesium grains, σ_{HP}. Substituting these values in Eq. (3), we have been able to determine the term $(1-f_{vrecr.})\,\sigma_{def.}$, corresponding to the strength contribution by the

remaining deformed magnesium grains. We have included the values of σ_{HP} and $\sigma_{def.}$ in Table 1 where we note that the stress, $\sigma_{def.}$, from the deformed grains is extremely high in the case of extruded material R18 and after six and eight ECAP passes at 300 °C. In Fig. 10 we have plotted, as bar charts, the corresponding strengthening contributions obtained from all the microstructural parameters for all the conditions. In Fig. 10a we show these values for the alloy in the cast state and after ECAP and we see that after 12 passes at 350 °C the contribution from deformed magnesium grains is small (16%) while the recrystallized grains contribute 34% to the yield stress. The material processed by six passes has a larger contribution from deformed grains (26%) as the fraction recrystallized is much smaller and those grains have a smaller strengthening contribution (21%). In all the four materials processed by ECAP in the as-cast state the largest contribution to the total strength is due to the LPSO particles (33–41%) since the longer exposure times at the higher temperature produce larger and more recovered microstructures in the magnesium matrix. In Fig. 10b we see the strengthening contributions in the as-extruded alloys at 350 °C and after ECAP at 300 °C. After 4–8 ECAP passes at 300 °C the deformed magnesium grains exhibit the largest contributions (44–46%) to the total yield stress of the materials, followed by similar contributions in both materials (20–25% each) from the recrystallized magnesium grains and the LPSO phase. In the case of the extruded R18 material, with a high value of $\sigma_{def.}$, the total strengthening contribution (31%) of the deformed grains is smaller than for the extruded R4 material or after ECAP due to the larger fraction of recrystallized grains which contribute 30% to the total of the yield stress.

Finally, it is worth noting that the present results confirm the effect of texture and its evolution on the ductility and strength of the different processed materials [7]. The materials with best ductilities (10%) are those with a large fraction of randomly oriented recrystallized grains while those with the highest strength have larger fraction of deformed grains with strong texture characterized by the basal planes being parallel to the extrusion/ECAP directions.

5. Conclusions

The microstructural changes taking place during extrusion and ECAP processing of a MgY_2Zn_1 alloy have been quantified in order to analyse the strengthening mechanisms that take place in the material. The following conclusions can be drawn:

- The as-cast microstructure, consisting of equiaxed magnesium dendrites and the LPSO phase distributed at the dendrite boundaries, becomes elongated by extrusion and ECAP due to the deformation of the LPSO phase which eventually cracks and comminutes. This comminution is more pronounced for the higher processing strains and lower temperature.
- In parallel, dynamic recrystallization of the magnesium matrix occurs resulting in a mixture of fine new magnesium grains and larger deformed grains. The fraction of DRX matrix is larger for the higher processing temperature and strains. The finest size of the new recrystallized grains was obtained after ECAP processing at 300 °C.
- Both extrusion and ECAP processing lead to an increase of mechanical strength of the alloy, with a maximum of 418 MPa being reached after eight ECAP passes at 300 °C. During processing at 350 °C, extrusion leads to higher strengthening for a lower equivalent strain, due to the much shorter exposure time at this temperature. A loss of ductility was observed on ECAP processing at 300 °C but not at 350 °C.
- The strengthening of the alloy has been analysed in terms of a composite consisting of a magnesium matrix and fiber-shaped LPSO phase particles. As the volume fraction of DRX magnesium increases, the new fine grains decrease in size and the remaining deformed grains become stronger, the alloy exhibits an increase in strength.
- It has been shown that materials processed by ECAP at 300 °C exhibit a larger contribution to strengthening from deformed magnesium grains. A larger contribution from the new recrystallized grains was obtained in materials processed at 350 °C, both after extrusion R18 and after 12 ECAP passes.
- We conclude that to optimize the strength a larger fraction of deformed magnesium grains is required, although this induces a lower ductility. A compromise in the exposure time during ECAP at intermediate temperatures (between 300–350 °C) could be reached, such that a larger fraction of recrystallized grains of the finer size (600 nm) might compensate a slightly lower fraction of deformed grains to maintain the highest strength with a ductility of around 5%.

Acknowledgements

We should like to acknowledge financial support of the Ministry of Economy and Competitiveness, Spain under Project number MAT2012-34135. We would like to acknowledge the expert support of Alfonso Garcia Delgado of the CENIM Microscopy Unit for assistance with electron microscopy studies and Miguel Acedo for assistance with casting and extrusion processing.

References

[1] A. Inoue, Y. Kawamura, M. Matsushita, K. Hayashi, J. Koike, J. Mater. Res. 16 (2001) 1894–1900.
[2] T. Itoi, K. Takahashi, H. Moriyama, M. Hirohashi, Scr. Mater. 59 (2008) 1155–1158.
[3] G. Garces, M. Maeso, I. Todd, P. Pérez, P. Adeva, J. Alloys Compd. 432 (2007) L10–L14.
[4] G. Garces, P. Pérez, S. Gonzalez, P. Adeva, Int. J. Mater. Res. 4 (2006) 404–408.
[5] M. Yamasaki, T. Anan, S. Yoshimoto, Y. Kawamura, Scr. Mater. 53 (2005) 799–803.
[6] Y. Kawamura, T. Kasahara, S. Izumi, M. Yamasaki, Scr. Mater. 55 (2006) 453–456.
[7] M. Yamasaki, K. Hashimoto, K. Hagihara, Y. Kawamura, Acta Mater. 59 (2011) 3646–3658.
[8] K. Hagihara, A. Kinoshita, Y. Sugino, M. Yamasaki, Y. Kawamura, H.Y. Yasuda, Y. Umakoshi, Acta Mater. 58 (2010) 6282–6293.
[9] Y. Kawamura, M. Yamasaki, Mater. Trans. 48 (2007) 2986–2992.
[10] S.B. Mi, Q.Q. Jin, Scr. Mater. 68 (2013) 635–638.
[11] G. Garces, E. Oñorbe, F. Dobes, P. Pérez, J.M. Antoranz, P. Adeva, Mater. Sci. Eng. A 539 (2012) 48–55.
[12] E. Oñorbe, G. Garces, F. Dobes, P. Pérez, P. Adeva, Metall. Mater. Trans. A 44 (2013) 2869–2883.
[13] Z.P. Luo, S.Q. Zhang, J. Mater., Sci. Lett. 19 (2000) 813–815.
[14] E. Abe, Y. Kawamura, K. Hayashi, A. Inoue, Acta Mater. 50 (2002) 3845–3857.
[15] Y.M. Zhu, A.J. Morton, J.F. Nie, Acta Mater. 58 (2010) 2936–2947.
[16] D. Egusa, E. Abe, Acta Mater. 60 (2012) 166–178.
[17] E. Oñorbe, G. Garces, P. Pérez, P. Adeva, J. Mater. Sci. 47 (2012) 1085–1093.
[18] E. Oñorbe, G. Garces, P. Pérez, S. Cabeza, M. Klaus, C. Genzel, E. Frutos, P. Adeva, Scr. Mater. 65 (2011) 719–722.
[19] R.Z. Valiev, T.G. Langdon, Prog. Mater. Sci. 51 (2006) 881–981.
[20] A.P. Zhilyaev, T.G. Langdon, Prog. Mater. Sci. 53 (2008) 893–979.
[21] D.G. Morris, M.A. Muñoz-Morris, Acta Mater. 50 (2002) 4047–4060.
[22] K. Valdés-León, M.A. Muñoz-Morris, D.G. Morris, Mater. Sci. Eng. A 536 (2012) 181–189.
[23] H. Watanabe, T. Mukai, S. Kamado, Y. Kojima, K. Higashi, Mater. Trans. 44 (2003) 463–467.
[24] M. Eddahbi, P. Pérez, M.A. Monge, G. Garcés, R. Pareja, P. Adeva, J. Alloys Compd. 473 (2009) 79–86.
[25] F.M. Lu, A.B. Ma, J.H. Jiang, D.H. Yang, Y.C. Yuan, L.Y. Zhang, J. Alloys Compd. 601 (2014) 140–145.
[26] J. Zhang, W. Zhang, L. Bian, W. Cheng, X. Niu, C. Xu, C.S. Wu, Mater. Sci. Eng. A 585 (2013) 268–276.
[27] J. Zhang, C. Chen, W. Cheng, L. Bian, H. Wang, C. Xu, Mater. Sci. Eng. A 559 (2013) 416–420.
[28] L. Fumin, M. Aibin, J. Jiang, D. Yang, D. Song, Y. Yuan, J. Chen, Mater. Sci. Eng. A 594 (2014) 330–333.
[29] Q. Yang, B.L. Xiao, Q. Zhang, M.Y. Zheng, Z.Y. Ma, Scr. Mater. 69 (2013) 801–804.
[30] J. Wang, Y. Iwahashi, Z. Horita, M. Furukawa, M. Nemoto, R.Z. Valiev, T.G. Langdon, Acta Mater. 44 (1996) 2973–2982.

[31] Y. Iwahashi, Z. Horita, M. Nemoto, T.G. Langdon, Acta Mater. 46 (1998) 3317–3331.
[32] A. Gholinia, P.B. Prangnell, M.V. Markushev, Acta Mater. 48 (2000) 1115–1130.
[33] M.A. Muñoz-Morris, N. Calderón, I. Gutierrez-Urrutia, D.G. Morris, Mater. Sci. Eng. A 425 (2006) 131–137.
[34] T. Itoi, T. Seimiya, Y. Kawamura, M. Hirohashi, Scr. Mater. 51 (2004) 107–111.
[35] M. Hirano, M. Yamasaki, K. Hagihara, K. Higashida, Y. Kawamura, Mater. Trans. 51 (2010) 1640–1647.
[36] P. Pérez, S. González, G. Garces, G. Caruana, P. Adeva, Mater. Sci. Eng. A 485 (2008) 194–199.
[37] S. Yoshimoto, M. Yamasaki, Y. Kawamura, Mater. Trans. 47 (2006) 959–965.
[38] T. Morikawa, K. Kaneko, K. Higashida, D. Kinoshita, M. Takenaka, Y. Kawamura, Mater. Trans. 49 (2008) 1294–1297.
[39] R. Matsumoto, M. Yamasaki, M. Otsu, Y. Kawamura, Mater. Trans. 50 (2009) 841–846.
[40] H.L. Cox, J. Appl. Phys. 3 (1952) 72–79.
[41] C.M. Landis, R.M. McMeeking, Compos. Sci. Technol. 59 (1999) 447–457.
[42] M. Kouzeli, A. Mortensen, Acta Mater. 50 (2002) 39–51.
[43] R.J. Arsenault, Acta Metall. 39 (1991) 47–57.
[44] G. Garces, M.A. Muñoz-Morris, D.G. Morris, J.A. Jimenez, P. Perez, P. Adeva, Intermetallics (2014) (accepted for publication).